Article

NMR-Based Analysis of Fluid Occurrence Space and Imbibition Oil Recovery in Gulong Shale

Fei Xu [1], Hanqiao Jiang [1]*, Ming Liu [1], Shuai Jiang [1], Yong Wang [1] and Junjian Li [1]

[1] State Key Laboratory of Petroleum Resources and Prospecting, China University of Petroleum (Beijing), Beijing 102249, China; 2020310133@student.cup.edu.cn

* Correspondence: jhqlf@163.com

Abstract: The Gulong shale oil reservoir is formed in freshwater to slightly saline lacustrine basins, mainly consisting of pure shale geological structure, which is quite different from other shale reservoirs around the world. Currently, the development of Gulong shale oil mainly relies on hydraulic fracturing, while the subsequent shut-in period for imbibition has been proven to be an effective method for enhancing shale oil recovery. To clarify the characteristics of fluid occurrence space and the variation of fluid occurrence during saltwater imbibition in Gulong shale, this paper carried out porosity and permeability tests on Gulong shale cores, and analyzed the fluid occurrence space characteristics and imbibition oil recovery based on nuclear magnetic resonance (NMR). In the porosity and permeability tests, the porosity measured by saturation method was calibrated using NMR T_2 spectra. Combined with the identification of fractures in shale cores using micro-CT and the analysis of porosity and permeability parameters, it was found that the permeability of shale cores was related to the development of fractures in shale cores. Through the testing and analysis of NMR T_1-T_2 two-dimensional spectra of the shale cores before and after saturation with oil, it was found that the shale mainly contains heavy oil, light oil, and clay-bound water, and they were distributed in different positions in the T_1-T_2 spectrum. Finally, the T_1-T_2 two-dimensional spectra of the shale core at different imbibition stages were analyzed, and it was found that the saltwater mainly entered the minuscule inorganic pores of clay minerals during the imbibition process, and squeezed the larger-sized inorganic pores containing light oil through the hydration expansion effect, thus expelling the light oil from the shale core and achieving the purpose of enhanced oil recovery.

Keywords: nuclear magnetic resonance; shale oil; occurrence space characteristics; imbibition

1. Introduction

With the increasingly growing demand for oil and gas resources worldwide, unconventional oil and gas resources are becoming increasingly important in global energy supply against the backdrop of sustained consumption of oil and gas resources and a gradual decrease in newly discovered conventional oil and gas reserves [1]. In recent years, with the sustained exploration of the Songliao Basin by the Daqing Oilfield, the huge development potential of the Gulong shale oil has been gradually tapped [2,3]. The Gulong shale oil is located in the Songliao Basin in Daqing, China, and belongs to the sedimentary deposits of freshwater to slightly brackish water lake basin. Its main body is pure shale geological structure [4-6]. The Gulong shale exhibits significant differences from other shale reservoirs around the world in terms of rock composition, physical properties, oil content, and shale oil mobility [7,8]. The reservoir space of the Gulong shale is mainly composed of matrix pores and bedding fractures, with the main types of pores being organic matter pores, dissolution pores, and interlayer pores of clay minerals. The nanoscale pore-throat system controlled by the horizontal bedding greatly improves the physical properties of the reservoir. Under the confining pressure condition, the horizontal permeability ranges from (0.011 to 1.620) ×10^{-3} μm^2, with an average of 0.580 ×10^{-3} μm^2. The Gulong shale is mainly composed of clay felsic shales, with an average clay mineral content of 35.6%. The main type of clay minerals in the Gulong shale is illite [9-11].

To evaluate the oil-bearing characteristics of the Gulong shale, previous studies have conducted NMR experiments. NMR is a non-destructive testing method that can accurately characterize the pore size distribution characteristics within the entire pore scale of the core through T_2 spectra. The T_2-D two-dimensional spectrum or T_1-T_2 two-dimensional spectrum can distinguish different types of fluids in the core [12,13]. Liu et al. [14] used NMR T_1-T_2 two-dimensional spectra to analyze the signals of organic matter, water, light hydrocarbons, and hydroxyl compounds in the Gulong shale, which clarified the oil saturation and movable oil saturation of the shale. However, the preservation process of the core before testing may inevitably result in the volatilization of light hydrocarbons, which has a certain impact on the results. Pang et al. [15] used NMR T_2 and T_1-T_2 spectra to analyze the pore size distribution and fluid composition in Gulong shale. However, their focus was mainly on the impact of fractures on oil saturation and fluid mobility, and did not provide a detailed classification of other fluids. In addition, Wei [16], Yan [17], and Li [18] have applied NMR technology to study the oil saturation, sensitivity of pore structure to external fluids, and other characteristics of the Gulong shale, respectively, achieving new insights into the Gulong shale and demonstrating the feasibility and effectiveness of NMR technology in shale analysis.

Currently, the main method of production for Gulong shale oil is through hydraulic fracturing, which yields light, high-quality crude oil with low density and viscosity [19]. During the shut-in period of the reservoir, significant improvement in shale oil production can be achieved through the mechanism of imbibition [20]. There is currently limited research on the imbibition of Gulong shale. Wu et al. [21] studied the imbibition and enhanced oil recovery effect of an emulsion system in Gulong shale, and the washing oil efficiency of imbibition can reach 54.6%. Liu et al. [22] conducted a spontaneous imbibition experiment on Gulong shale cores and found that the oil recovery tended to stabilize after 100 hours. The above studies indicate that imbibition is an important way to improve the recovery of shale oil. But the oil-water displacement process during the imbibition of Gulong shale is not clear yet, and the variation of fluids distribution in different pore sizes of shale under imbibition require further study.

To analyze the occurrence space characteristics of different fluids, especially the oil phase, and the variation of fluids distribution in the core during the imbibition process, this paper intends to conduct relevant research using NMR technology. First, conventional core experiments will be carried out to analyze the porosity and permeability characteristics and fracture development of the Gulong shale core samples. To avoid damage to the organic pores of the shale by washing oil, the dry rock samples that have not been treated in any way will be directly saturated with kerosene, and the porosity measured by the saturation method will be corrected based on the T_2 spectrum values of the core before and after oil saturation. Next, by measuring and analyzing the NMR T_1-T_2 two-dimensional spectra of the shale core before and after oil saturation, the occurrence space characteristics of the fluids in the shale, especially the oil phase, will be studied. Finally, a saltwater imbibition experiment will be performed on the shale core, and the variation of fluids distribution during the imbibition process will be studied and analyzed by measuring the NMR T_1-T_2 two-dimensional spectra at different imbibition times.

2. Experiment Apparatus and Materials

2.1 Experiment Apparatus

In this experiment, the gas permeability of Gulong shale core was measured using the PDP-200 pulse decay permeameters. The permeability measurement range of the apparatus is 10^{-5}-10mD, and the maximum confining pressure of the core holder can reach 70 MPa, which can simulate the overburden pressure of most oil and gas reservoirs and meet the requirements of this experiment. The dry shale samples were saturated with kerosene using a conventional saturation device. By comparing the difference in the weight and T_2 spectrum signal value of the core before and after saturation with oil, the accurate porosity of the shale was calculated. The SPEC-023 Nuclear Magnetic Resonance flow experiment analyzer was used to measure the T_2 spectra and T_1-T_2 two-dimensional spectra of the Gulong shale cores in the dry and saturated oil states. The magnetic field frequency of

the instrument was 9.38 MHz, and the experimental parameters were set as follows: sampling interval of 1 us, number of echo of 1024, echo time of 120 us, waiting time of 2500 ms, TIMin of 100 us, and TIMax of 1.5 s. Conventional imbibition bottle was used to conduct shale imbibition experiments after saturation with oil.

2.2 Experiment Materials

Three pieces of dry Gulong shale cores are shown in Figure 1, with the top and bottom surfaces left exposed and the side of the cylindrical cores wrapped in thermoplastic tubing to protect the shale cores from breaking. Kerosene is used to saturate dry rock cores. KCl solution is used for conducting the imbibition experiments on the Gulong shale cores with oil saturated. The salinity of the KCl solution is 6000 ppm, consistent with the salinity of the fluid in a shale reservoir in Daqing.

Figure 1. Photograph of the Gulong Shale.

3. Experimental Principle and Method

3.1. Experimental Principle

The main principle of one-dimensional NMR can be described by the following equation:

$$\frac{1}{T_{2a}} = \frac{1}{T_{2b}} + \rho\frac{s}{v} \tag{1}$$

where T_{2b} is the intrinsic relaxation time of the fluid, ms; T_{2a} is the measured apparent relaxation time in the shale core, ms; ρ is the surface relaxation rate of the fluid in the pore, m/s; $\frac{s}{v}$ is the surface area to volume ratio of the fluid in the pore, μm^{-1}, which is inversely proportional to the pore size.

For fluids with long intrinsic relaxation time T_{2b}, such as water and light oil, $\frac{1}{T_{2b}} \ll \rho\frac{s}{v}$, T_{2a} is mainly determined by $\rho\frac{s}{v}$, so the one-dimensional NMR spectrum can reflect the distribution of fluids in the internal pores.

Conventional cores need to be cleaned and dried before measuring their permeability and porosity. However, shale cores differ from conventional cores. Organic matter in shale, such as kerogen, can dissolve in the organic solvent used for cleaning, which can cause irreversible damage to the organic pores in the shale if cleaned. Therefore, in order to accurately measure the porosity of unwashed shale, it is necessary to measure the residual oil and bound water content inside the shale.

The total signal intensity of NMR T_2 spectrum was positively correlated with fluid content, and the higher the fluid content in shale samples, the greater the total T_2 signal value. The total signal value of T_2 spectrum obtained from the dry scan, S_1, and that obtained from the saturated shale after being saturated with kerosene, S_2, were related to the volume of residual oil and bound water in the dry shale sample, V_1, and the volume of kerosene that saturated the shale, V_{kero}, by the following equations:

$$\frac{S_1}{S_2} = \frac{V_1}{V_1 + V_{\text{kero}}} \tag{2}$$

Therefore, we have the following relationship:

$$V_1 = \frac{S_1}{S_2 - S_1} V_{\text{kero}} \tag{3}$$

The corrected porosity by NMR can be obtained as follows:

$$\phi_{\text{cor}} = \frac{V_1 + V_{\text{kero}}}{V_{\text{shale}}} = \frac{\frac{S_1}{S_2 - S_1} V_{\text{kero}} + V_{\text{kero}}}{V_{\text{shale}}} = \frac{S_2}{S_2 - S_1} \frac{V_{\text{kero}}}{V_{\text{shale}}} = \frac{S_2 (m_2 - m_1)}{(S_2 - S_1) \rho_{\text{o}} V_{\text{shale}}} \tag{4}$$

where m_1 is the dry core sample mass, m_2 is the saturated core sample mass with oil, S_1 is the total signal value of T_2 spectrum of dry core, S_2 is the total signal value of T_2 spectrum of oil-saturated core, ρ_o is the density of kerosene, and V_{shale} is the volume of the shale sample.

Core NMR analysis can be done in two ways: T_2-D and T_1-T_2 spectra. Studies on T_2-D two-dimensional spectrum analysis of rock cores mainly focus on sandstones, where the diffusion characteristics of fluids are reflected by varying the echo time T_E over a wide range. The T_E value determines the accuracy of measuring the pore size, with smaller T_E values allowing for measurement of smaller pores. In shale, where nanometer-scale pores dominate, a small T_E value is required to ensure measurement accuracy. However, the T_2-D two-dimensional spectrum cannot guarantee a consistently small T_E, making it difficult to meet the precision requirements of nanometer-scale pores in shale measurements. Therefore, T_2-D two-dimensional spectrum is only suitable for conventional reservoirs and cannot accurately evaluate shale. When measuring the T_1-T_2 two-dimensional spectrum, it is necessary to ensure that the echo spacing T_E is a small value, thereby ignoring the influence of diffusion coefficient D. This property just meets the measurement requirements of nanometer-scale pores in shale, so T_1-T_2 two-dimensional spectrum can more accurately evaluate shale.

3.2 Experimental Method

3.2.1 Measurement of Permeability in Shale Core

The gas permeability experiment uses the PDP-200 pulse decay permeameters from Core Lab laboratory in the United States to measure ultra-low permeability. The experimental apparatus is shown in Figure 2. Experimental procedure is as follows: (1) Preheat the PDP equipment and check the airtightness of the apparatus; (2) Perform a test on a mock core to detect system errors; (3) Place the Gulong shale core into the apparatus, apply a confining pressure of 30 MPa, and conduct nitrogen gas permeability test; (4) Analyze the data using software to obtain the permeability value. Applying a confining pressure of 30 MPa simulates the pressure environment of shale in actual formations. If not, the low confinement pressure would result in lower closure of fractures in shale, which would affect the accuracy of shale permeability measurement.

Figure 2. PDP-200 pulse decay permeameters.

3.2.2 Saturation of shale core with kerosene.

To ensure the shale core is fully saturated with kerosene, it is necessary to conduct long-term vacuum and high-pressure saturation experiments on the shale core with kerosene. Experimental procedure is as follows: (1) Check the leakage of the instrument pipeline; (2) Place the three shale cores in the pressure vessel and evacuate for 15 days to achieve a vacuum degree of 0.1 Pa, ensuring that the shale cores are fully evacuated; (3) Saturate the shale cores with kerosene under a pressure of 30 MPa for 15 days, ensuring that the shale is fully saturated with kerosene.

3.2.3 Shale Imbibition Experiment

After preparing a 6000 ppm KCl solution with deionized water, the Gulong shale cores saturated with kerosene were placed into the imbibition bottle. At regular intervals, the cores were removed and wiped clean of both water and oil. Then, the weight was recorded, and the NMR T_2 spectra and T_1-T_2 two-dimensional spectra were measured.

3.2.4 NMR spectrum testing

The dry cores, kerosene-saturated cores, and the core taken out after each interval during the imbibition process were measured for T_2 spectrum and T_1-T_2 two-dimensional spectrum using SPEC-023 Nuclear Magnetic Resonance Permeameter. The T_2 spectrum data were recorded and the T_1-T_2 two-dimensional spectra were generated by using the particular software.

4. Result and discussion.

*4.1 Analysis of porosity and permeability*

The permeability of the three shale cores measured by the PDP-200 pulse decay permeameters and the porosity of the cores calculated from the changes in the shale core mass before and after saturation with oil were shown in Table 1. The porosity and permeability of Core 1# were both the highest among the three cores. Cores 2# and Cores 3# had similar porosity, but their permeability differed significantly. The permeability of core No.2 was about three times that of core 3#.

**Table 1.** Porosity and Permeability Parameters of Gulong Shale Core Samples

Core number	Dry weight /g	Weight after saturation /g	Volume of kerosene /cm³	Core volume /cm³	Porosity /%	Permeability /mD
1#	27.22	27.895	0.84	10.47	8.06	0.422
2#	75.786	77.218	1.79	28.43	6.30	0.235
3#	61.794	62.951	1.45	23.44	6.17	0.080

Due to the presence of bound water or heavy oil that was difficult to evaporate in the dry core sample, the porosity measured above did not take into account the residual fluids in the core. Therefore, the NMR T_2 spectrum was used below to correct the porosity.
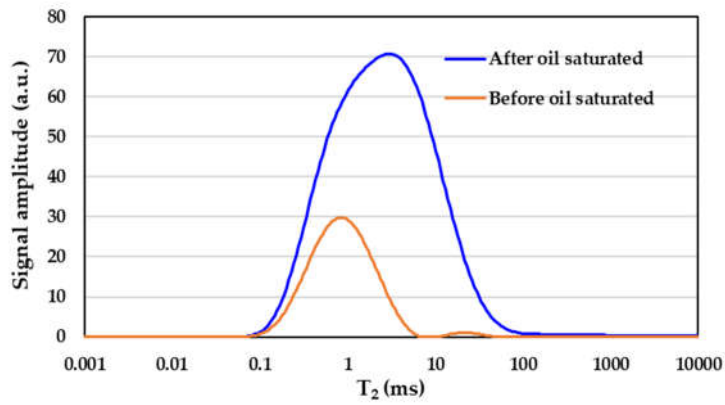
The NMR T_2 spectra of three shale cores before and after saturation with oil were shown in Figure 3:
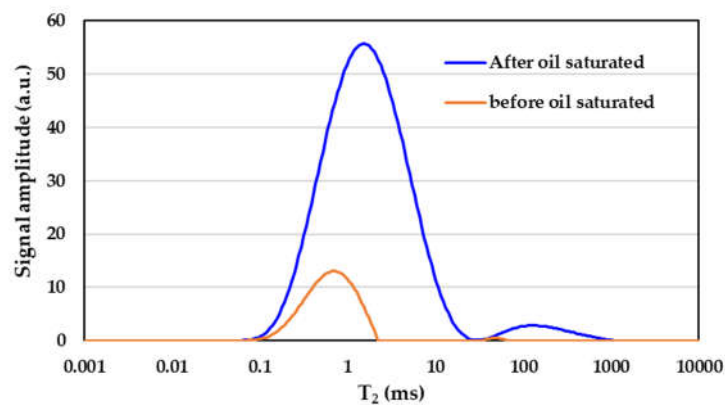
(a) NMR T_2 spectrum curve for Core 1#
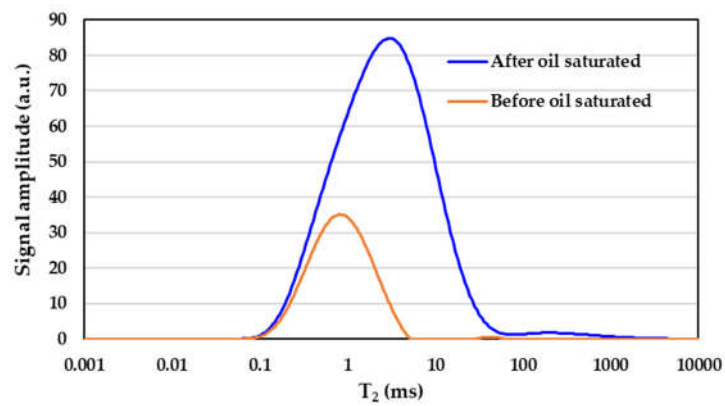
(b) NMR T_2 spectrum curve for Core 2#

(c) NMR T_2 spectrum curve for Core 3#

**Figure 3.** NMR T_2 spectrum curves of Gulong shale cores.

The porosity corrected based on the NMR T_2 spectra was shown in Table 2.

Table 2. Corrected porosity of Gulong shale cores

Core number	The ratio of T_2 spectral signals before and after saturation	Uncorrected porosity	Corrected porosity	Porosity increment	Permeability /mD
1#	0.143	8.06%	9.40%	1.34%	0.422
2#	0.267	6.30%	8.59%	2.29%	0.235
3#	0.25	6.17%	8.23%	2.06%	0.080

Comparison of the corrected porosity and permeability of the rock cores showed that the porosity of Core 1# was still the highest, but only 0.81% higher than Core 2# and 1.17% higher than Core 3#. However, the permeability of Core 1 was significantly higher than that of Core 2# and Core 3#. Moreover, while the porosity of Core 2# was only 0.36% higher than that of Core 3#, the permeability of Core 2# was about three times that of Core 3#. To analyze the reasons for the differences in porosity and permeability mentioned above, micro-CT scanning was conducted on the three cores, and the imaging results were shown in Figure 4. Due to equipment limitations, the scanning height of each core was only about 2cm, while the scanning width was the cross-section diameter of the core, which was 2.5 cm.

Micro-CT can identify fluids in the pores of the cores, but it can only identify fluids in micrometer-sized pores. Since the pores in Gulong shale are mostly nanometer-sized, it is impossible to identify fluids in the pores of the shale cores using Micro-CT. However, the fractures in the shale are on a micrometer scale and the fluid in the fractures can be identified by micro-CT scanning. As can be seen from Figure 4, the left half of the micro-CT scanning image of the Core 1# showed an obvious vertically fracture, the middle of the micro-CT scanning image of the Core 2# core showed an obvious meandering fracture, and there was no trace of fractures in the micro-CT scanning image of Core 3#. These micro-CT scan images explained why Core 3# has the lowest permeability and Core 1# and Core 2# had much higher permeability than Core 3#. Otherwise, the NMR T_2 spectra of the shale cores with oil saturated in Figure 3 could also tell if there were fractures in the cores. It could be seen that Core 1# had a clear peak around T_2 value of 100ms, which was the signal of oil phase in the fracture. Core 2# also had a small peak around T_2 value of 100-1000ms, with a peak value significantly smaller than that of Core 1#, indicating that the fracture volume of Core 2# as smaller than that of Core 1#, and the fracture of Core 1# was more developed. So that the permeability of Core 1# was higher than that of Core 2#. Core 3# had almost no peak around T_2 value of 100-1000ms, indicating that there was no fracture development in Core 3#. Therefore, the permeability of shale was significantly correlated with the development of fractures, i.e. the more developed the fracture was, the higher the permeability of the shale was.

(a) Core 1#   (b) Core 2#   (c) Core 3#
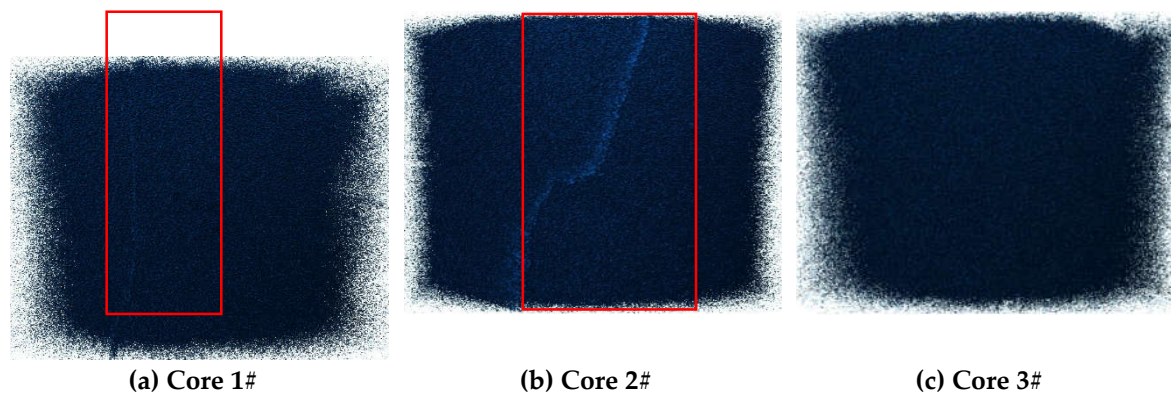
Figure 4. Micro-CT scan images of the Gulong shale core.

4.2 Fluid occurrence space analysis

The distribution of fluids within the shale cores was analyzed using the results of T_1-T_2 spectrum tests on the cores before and after saturation with oil. The T_1-T_2 spectra of the Core 1# before and after saturation with oil were shown in Figure 5.
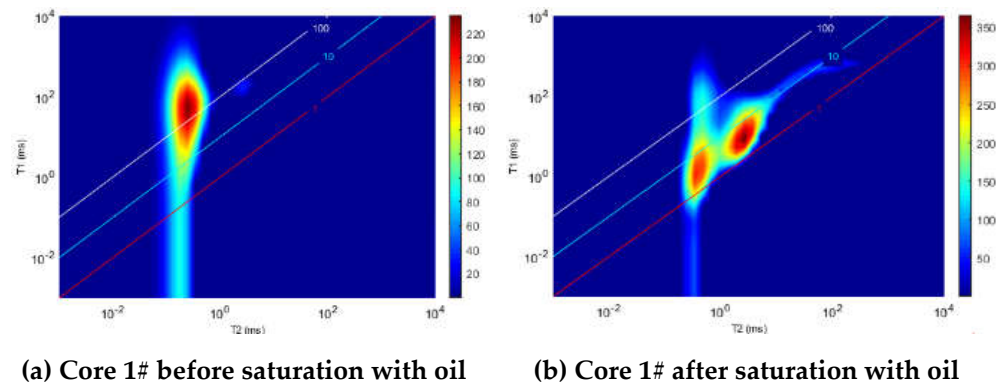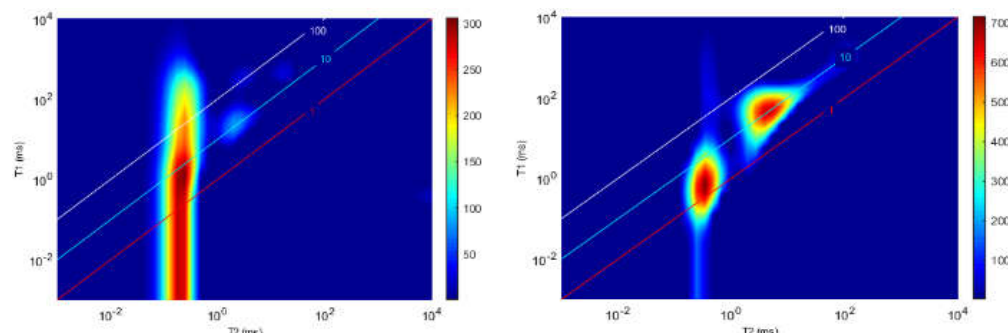

(a) Core 1# before saturation with oil   (b) Core 1# after saturation with oil

Figure 5. The comparison of the T_1-T_2 spectra of Core 1# before and after being saturated with oil.

As shown in Figure 5a, the T_1-T_2 spectra of Core 1# in its dry state had only one peak signal area in red. The signals from fluids in this area were mainly distributed in the T_2 range of around 0.1-1ms and the T_1/T_2 range of around 100. This indicated that the fluids present in the Core 1# before oil saturation were mainly heavy oil components such as asphaltene. As shown in Figure 5b, after saturation with oil, two red peak signal areas appeared in the T_1-T_2 spectrum, with T_2 ranges of approximately 0.1-1ms and 1-10ms, respectively, both of which were distributed in the T_1/T_2 range of 1-10. Since the pores in shale that contained oil were mainly organic and inorganic pores, and the pore size of organic pores was usually smaller than that of inorganic pores [14-18], it could be inferred that the left red peak signal area corresponded to the oil phase saturated in the organic pores, while the right red peak signal area corresponded to the oil phase saturated in the inorganic pores. In addition, in the T_1-T_2 spectrum after oil saturation, there were light blue signals appearing in the region with T_2 values of around 100-1000ms and T_1/T_2 values of around 10, which mainly corresponded to the signals of the oil phase in the shale fractures. This indicated that the proportion of oil phase in the fractures of the shale rock core was very low.

The T_1-T_2 spectra of Core 2# before and after oil saturation were shown in Figure 6. As shown in Figure 6a, it could be seen that the T_1-T_2 spectrum of Core 2# in the dry state had a red bar-shaped signal region, and the signals of the fluids in this region were distributed in the T_2 value range of about 0.1-1ms and the T_1/T_2 value range below 10, indicating that the fluids in Core 2# before oil saturation were mainly composed of clay-bound water and light oil components in organic pores. According to Figure 6b, after saturation with oil, the two red peak signal areas appeared in the T_1-T_2 spectrum, with T_2 values ranging from approximately 0.1-1ms and 1-10ms, and T_1/T_2 values ranging from approximately 1-10 and near 10, respectively, which was similar to the trend observed in Core 1#.

(a) Core 2# before saturation with oil   (b) Core 2# after saturation with oil

Figure 6. The comparison of the T_1-T_2 spectra of Core 2# before and after being saturated with oil.

The T_1-T_2 spectra of Core 3# before and after saturation with oil were shown in Figure 7. From Figure 7a, it could be seen that the dry state T_1-T_2 spectrum of Core 3# also had a red bar-shaped signal area, and the signals of the fluid stored in this area were distributed almost throughout the T_2 value range of about 0.1-1ms, indicating that the fluids contained in Core 3# before oil saturation included heavy and light oil components in organic pores, as well as clay-bound water. According to Figure 7b, after being saturated with oil, two red peak signal areas appeared in the T_1-T_2 spectrum. The T_2 value ranges of these areas were about 0.1-1ms and 1-10ms, respectively, and the T_1/T_2 values were between 1-10 and around 10, which was similar to the pattern of the first two cores. In addition, in the T_1-T_2 spectrum after oil saturation, in the region where T_1/T_2 was about 10 and T_2 value is around 100-1000ms, the fluid signal of Core 3# was much weaker than that of Core 1# and slightly weaker than that of Core 2#, indicating that Core 3# was basically not developed with fractures, consistent with the micro-CT scanning results mentioned earlier.
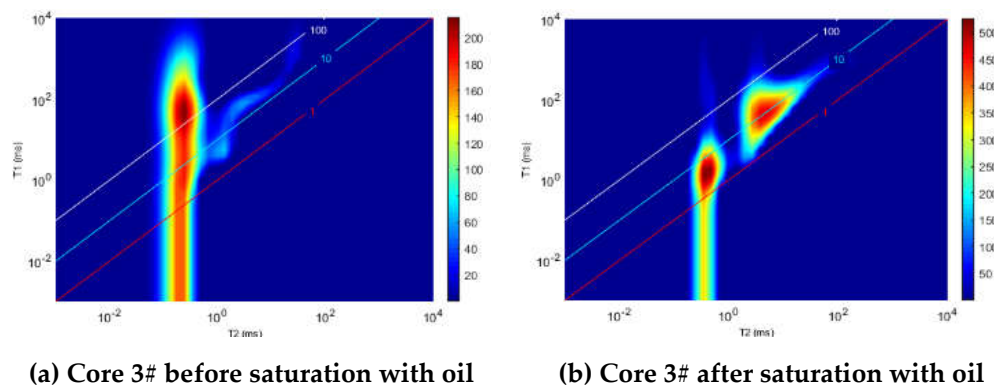

(a) Core 3# before saturation with oil   (b) Core 3# after saturation with oil

Figure 7. The comparison of the T_1-T_2 spectra of Core 3# before and after being saturated with oil.

Analysis of the NMR T_1-T_2 spectra of the three shale cores before and after oil saturation indicated that the fluid types in the Gulong shale cores in this experiment mainly included heavy oil, light oil, and clay-bound water. Heavy oil was mainly distributed in organic pores, while light oil was distributed in both organic pores, inorganic pores, and fractures. The organic pores mainly distributed in the T_2 value range of 0.1-1ms in the T_1-T_2 spectrum, and the heavy oil in the organic pores was distributed around T_1/T_2 value of 100, while the light oil in the organic pores was distributed in the T_1/T_2 value range of 1-10. The light oil in the inorganic pores distributed in the T_2 value range of 1-100ms and around a T_1/T_2 value of 10. The clay-bound water was mainly distributed in the T_2 range of 0.1-1ms, and its signal was mainly located around a T_1/T_2 value of 1.

4.3 Analysis of the imbibition effect

To investigate the effect of saltwater imbibition on the oil mobilization and fluid distribution in the Gulong shale core, a 120-hour imbibition experiment with 6000 ppm KCl solution was conducted on Core 3#. During the imbibition process, the core was removed multiple times for weighing and T_1-T_2 spectrum measurement. During the imbibition process, it was observed that the core released oil, as shown in Figure 8.

Figure 8. Expulsion of oil from the core during the imbibition process.

Using the mass difference of the Core 3# obtained by weighing at each time, the approximate amount of oil extracted by imbibition can be calculated. The recovery rate curve of Core 3# during the imbibition process was then plotted, as shown in Figure 9. Due to the wiping of the core before weighing, the calculated results had some errors, leading to negative oil recovery values in the early stage of imbibition. As the duration of the imbibition increased, the water phase was gradually imbibed into the core and displaced the oil phase, resulting in a positive and gradual increase of the recovery. The imbibition rate decreased gradually as the imbibition time increased, with the fastest imbibition rate at the beginning and the slowest at the end. At the end of the 120-hour imbibition experiment, the imbibition recovery rate reached 36.6%.
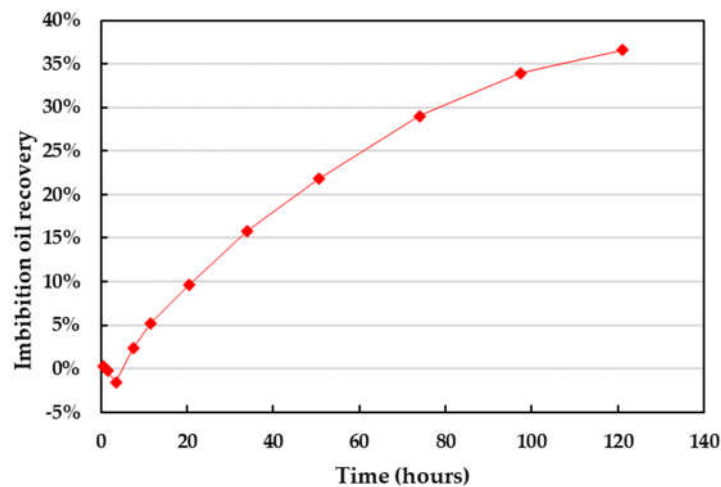

Figure 9. Imbibition oil recovery curve of Core 3#.

The results of T_1-T_2 two-dimensional spectrum tests of the shale core at different imbibition times were shown in Figure 10. With the increase of imbibition time, the color of the signal peak in the area where the clay-bound water was present, i.e. the range of T_2 values of 0.1-1 ms and T_1/T_2 values near 1, gradually changed from light yellow to dark red, indicating that the signal value was continuously increasing.
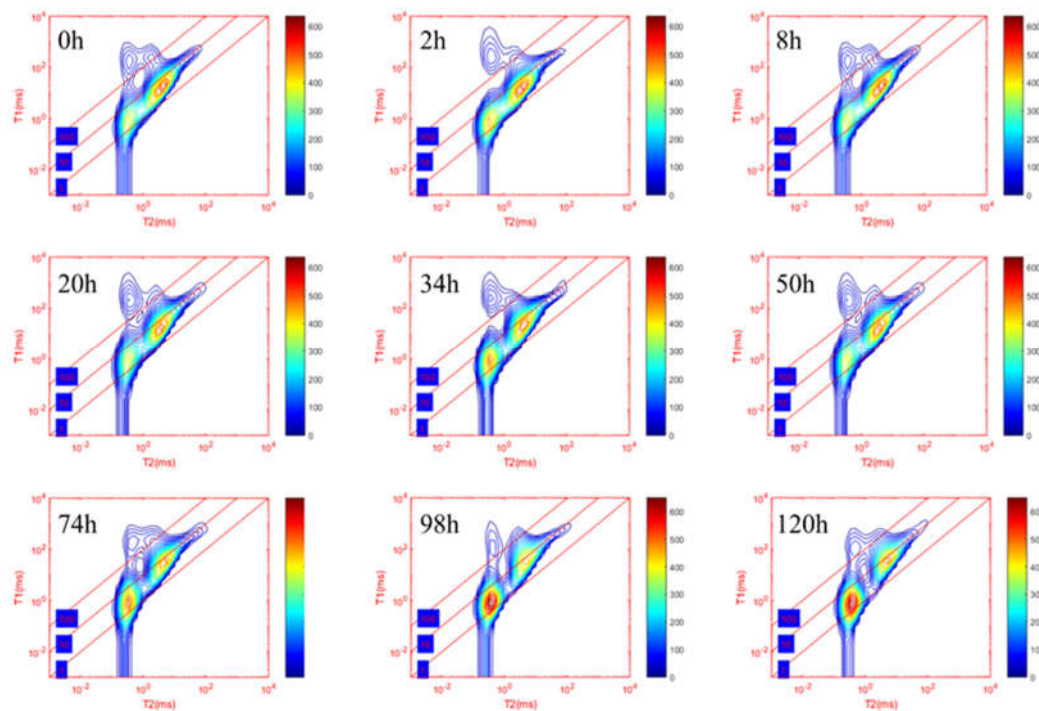
Figure 10. T_1-T_2 spectra on shale core under different imbibition times.

On the other hand, the color of the signal peak in the area where light oil in inorganic pores was present, i.e. the range of T_2 values of 1-100 ms and T_1/T_2 values near 10, changed from red to yellow, indicating that the signal value in this area was continuously decreasing with the increase of imbibition time. In addition, it was worth noting that the oil signals in the vicinity of T_2 value of 1 also continuously weaken with the progress of the imbibition, and the signal values were basically reduced to zero at the end of the imbibition. The above phenomenon indicated that the saltwater imbibition into the core mainly entered the minuscule inorganic pores of clay minerals, thus reinforcing the clay-bound water signal. The light oil in the larger inorganic pores was expelled because the clay minerals would undergo a certain degree of hydration expansion after the saltwater entered the minuscule clay mineral inorganic pores, thus squeezing the larger pores and forcing the oil phase in them to be expelled. The small-sized inorganic pores containing oil phase were fully squeezed by the hydration expansion effect, and most of the oil phase was expelled, which caused the oil phase signal near T_2 value of 1 to be reduced to almost zero at the end of the imbibition process. The signal of light oil in the organic pores overlapped with that of the water phase, and the signal value kept increasing, making it difficult to determine whether the light oil in the organic pores has been mobilized. However, considering that mobilizing the oil in the organic pores was the most difficult and that the organic pores are oleophilic, it was inferred that the light oil in the organic pores was not mobilized or was only slightly mobilized. Therefore, the oil extracted by saltwater imbibition mainly came from the oil in the inorganic pores.

4. Conclusions

In this study, the pore and permeability characteristics, the fluid occurrence space and saltwater imbibition oil recovery characteristics of the Gulong shale cores were studied using NMR. The conclusions are as follows:

(1) The porosity and permeability characteristics of the Gulong shale cores were analyzed using NMR T_2 spectra. This method could accurately measure the porosity without oil washing, thus avoiding the destruction of organic matter in shale cores. In the case of similar porosities, the

permeability of the Gulong shale core was related to the degree of fracture development, with greater fracture development resulting in higher permeability.

(2) The fluid types in the Gulong shale cores measured in this experiment mainly included heavy oil, light oil, and clay-bound water, with light oil being further divided into organic pore light oil and inorganic pore light oil. Among these fluid types, except for the partial overlap of the distribution areas of clay-bound water and organic pore light oil in the NMR T_1-T_2 spectra, heavy oil and inorganic pore light oil were distributed in different regions in the NMR T_1-T_2 spectra.

(3) Saltwater imbibition could remove a certain amount of oil from the shale core. Combined with the NMR T_1-T_2 spectrum, it was known that during the process of imbibition, saltwater mainly entered the minuscule inorganic pores of clay minerals under the action of capillary force, and after undergoing hydration expansion, it squeezed the inorganic pores, thereby removing the light oil in the inorganic pores. The oil phase in the organic pores was rarely affected.

Reference:

1. Zou, C.; Dong, D.; Wang, Y.; Li, X.; Huang, J.; Wang, S.; Guan, Q.; Zhang, C.; Wang, H.; Liu, H. Shale Gas in China: Characteristics, Challenges and Prospects (II). Petrol. Explor. Develop. **2016**, *43*,182-196.
2. Li, Y.; Zhao, Q.; Qi, L.; Xue, Z.; Cao.; Liu, Z. Evaluation technology and practice of continental shale oil development in China. Petrol. Explor. Develop. **2022**, *49*, 1098-1109.
3. Liu, B.; Shi, J.; Fu X.; Yanfang, Lyu Y.; Sun, X.; Gong, L.; Bai Y. Petrological characteristics and shale oil enrichment of lacustrine fine-grained sedimentary system: A case study of organic-rich shale in first member of Cretaceous Qingshankou Formation in Gulong Sag, Songliao Basin, NE China. Petrol. Explor. Develop. **2018**, *45*, 884-897.
4. Li C.; Yan, W.; Wu, H.; Han, T.; Zheng, J.; Jun, Y.; Zhou, F.; Xu, H. Calculation of oil saturation in clay-rich shale reservoirs: A case study of Qing 1 Member of Cretaceous Qingshankou Formation in Gulong Sag, Songliao Basin, NE Chin. Petrol. Explor. Develop. **2023**, *49*, 1351-1363.
5. Hua, G.; Wu, S.; Zhang, J.; Liu, R.; Guan, M.; Cai, Y.; Li, M.; Zhang, S. Laminar Structure and Reservoir Quality of Shales with High Clay Mineral Content in the Qingshankou Formation, Songliao Basin. Energies, **2022**, *15*, 6132.
6. Liu, B.; Wang, H.; Fu, X.; Bai, Y.; Bai, L.; Jia, M.; He, B. Lithofacies and depositional setting of a highly prospective lacustrine shale oil succession from the Upper Cretaceous Qingshankou Formation in the Gulong sag, northern Songliao Basin, northeast China. AAPG Bull. **2019**, *103*, 405-432.
7. Niu, D.; Li, Y.; Zhang, Y.; Sun, P.; Wu, H.; Fu, H.; Wang, Z. Multi-scale classification and evaluation of shale reservoirs and 'sweet spot' prediction of the second and third members of the Qingshankou Formation in the Songliao Basin based on machine learning. J. Pet. Sci. Eng. **2022**, *216*, 110678.
8. Li, S.; Li, S.; Guo, R.; Zhou, X.; Wang, Y.; Chen, J.; Zhang, J.; Hao, L.; Ma, .; Qiu, J. Occurrence State of Soluble Organic Matter in Shale Oil Reservoirs from the Upper Triassic Yanchang Formation in the Ordos Basin, China: Insights from Multipolarity Sequential Extraction. Nat. Resour. Res. **2021**, *30*: 4379-402.
9. Sun, L.; Liu, H.; He, W.; Li, G.; Zhang, S.; Zhu, R.; Jin, X.; Meng. S.; Jiang, H. (2021). An analysis of major scientific problems and research paths of Gulong shale oil in daqing oilfield, ne china. Petrol. Explor. Develop. **2021**, *48*, 527-540.
10. He, W.; Wang, M.; Wang, X.; Meng, Q.; Wu, Y.; Lin, T.; Li, J.; Zhang, J. Pore Structure Characteristics and Affecting Factors of Shale in the First Member of the Qingshankou Formation in the Gulong Sag, Songliao Basin. ACS Omega **2022**, *7*, 35755-35773.
11. Huo, Z.; Hao, S.; Liu, B.; Zhang, J.; Ding, J.; Tang, X.; Li, .; Yu, X. Geochemical characteristics and hydrocarbon expulsion of source rocks in the first member of the Qingshankou Formation in the Qijia-Gulong Sag, Songliao Basin, Northeast China: Evaluation of shale oil resource potential. Energy Sci. Eng. **2020**, *8*, 1450-1467.
12. Zhong, J.; Yan, R.; Zhang, H.; Feng, Y.; Liu, X.. A decomposition method of nuclear magnetic resonance t2 spectrum for identifying fluid properties. Petrol. Explor. Develop. **2020**, *47*, 740-752.

13.   Liu, Z.; Liu, D.; Cai, Y.; Yao, Y.; Pan, Z.; Zhou, Y. Application of nuclear magnetic resonance (NMR) in coalbed methane and shale reservoirs: A review. Int. J. Coal Geol. **2020**, *218*, 103261.

14.   Liu, B.; Bai, L.; Chi, Y.; Jia, R.; Fu.; Yang, L. Geochemical characterization and quantitative evaluation of shale oil reservoir by two-dimensional nuclear magnetic resonance and quantitative grain fluorescence on extract: A case study from the Qingshankou Formation in Southern Songliao Basin, northeast China. Mar. Pet. Geol. **2020**, *120*, 104481.

15.   Pang, X.; Wang, G.; Kuang, L.; Zhao, F.; Li, C.; Wang, C.; Zhang, M.; Lai, J. Lamellation fractures in shale oil reservoirs: Recognition, prediction and their influence on oil enrichment. Mar. Pet. Geol. **2022**, *148*, 106032.

16.   Wei J.; Fu L.; Zhao G.; Li B.; Zhao X.; Wang A. Sensitivity of shale pore structure to external fluids for Gulong shaleoil reservoir in Songliao Basin. Pet. Geol. Oilfield Dev. Daqing **2022**, *41*, 120-129.

17.   Yan W.; Zhang Z.; Chen L.; Zhao Z.; Wang W. New evaluating method of oil saturation in Gulong shalebased on NMR technique. Pet. Geol. Oilfield Dev. Daqing **2021**, *40*, 78-86.

18.   Li B.; Deng S.; Liu Y.; Cao S.; Jin D.; Dong D. Measurement method of movable fluid saturation ofGulong shale oil reservoir in Songliao Basin. Pet. Geol. Oilfield Dev. Daqing **2022**, *41*, 130-138.

19.   He, W.; Meng, Q.; Feng, Z.; Zhang, J.; Wang, R. In-situ accumulation theory and exploration &development practice of Gulong shale oil in Songliao Basin. Acta Pet. Sin. **2022**, *43*, 1-14.

20.   He, W.; Liu, B.; Zhang, J.; Bai, L.; Tian, S.; Chi, Y. Geological Characteristics and Key Scientific and Technological Problems of Gulong Shale Oil in Songliao Basin. Earth Sci. **2023**, *48*, 49-62.

21.   Wu, X.; Hou, Z.; Yang, Y.; Chen J.; Wang, H.; Nie, C. Development and performance evaluation for Gulong 1# emulsion system. Pet. Geol. Oilfield Dev. Daqing **2022**, *41*, 112-119.

22.   Liu G.; Yang D.; Mei X.; Yu S.; Ma W.; Fan X. Method of well-soaking and controlled flowback after large-scalefracturing of Gulong shale oil reserviors in Songliao Basin. Pet. Geol. Oilfield Dev. Daqing **2020**, *39*, 147-154.